

Theoretical model of the interactions between Ca^{2+} , calmodulin and myosin light chain kinase

Aleš Fajmut^{a,*}, Milan Brumen^{a,b}, Stefan Schuster^c

^a Department of Physics, Medical Faculty and Faculty of Education, University of Maribor, Slomškov trg 15, SI-2000 Maribor, Slovenia

^b Institute Jožef Stefan, Jamova 39, SI- Ljubljana, Slovenia

^c Department of Bioinformatics, Faculty of Biology and Pharmaceutics, Friedrich Schiller University Jena, Ernst-Abbe-Platz 2, D-07743 Jena, Germany

Received 17 March 2005; revised 15 June 2005; accepted 29 June 2005

Available online 19 July 2005

Edited by Judit Ovadi

Abstract Active Ca^{2+} /calmodulin (CaM)-dependent myosin light chain kinase (MLCK) plays an important role in the process of MLC phosphorylation and consecutive smooth muscle contraction. Here, we propose a mathematical model of a detailed kinetic scheme describing interactions among Ca^{2+} , CaM and MLCK and taking into account eight different aggregates. The main model result is the prediction of the Ca^{2+} dependent active form of MLCK, which is in the model taken as proportional to the concentration of $\text{Ca}_4\text{CaM} \cdot \text{MLCK}$ complex. Wegscheider's condition is additionally applied as a constraint enabling the prediction of some parameter values that have not yet been obtained by experiments.

© 2005 Published by Elsevier B.V. on behalf of the Federation of European Biochemical Societies.

Keywords: Calcium; Calmodulin; Myosin light chain kinase; Mathematical model

1. Introduction

Activation of myosin light chain kinase (MLCK) by the Ca^{2+} /calmodulin (CaM) complex affects the phosphorylation of the myosin light chain (MLC). MLC has an important role in smooth muscle contraction and other cellular processes linked to secretion and contraction [1]. According to a generally accepted theory an increase in cytosolic Ca^{2+} concentration ($[\text{Ca}^{2+}]$) initiates Ca^{2+} binding to four binding sites of CaM. Then the Ca_4CaM complex interacts with MLCK [2,3]. According to experimental results, the activity of MLCK determines the rate and extent of MLC phosphorylation, which in turn results in a greater velocity of contraction due to an increase in the actin–myosin cross bridge cycling rate [4–6]. More rapid contraction of the airway smooth muscle has been suggested as an explanation for clinically evident impairment of normal stretch-induced relaxation in asthmatics [7].

Based on recent experimental results, it has been suggested that not only Ca_4CaM but also Ca^{2+} -free CaM or Ca_2CaM complexes can interact with MLCK [8,9]. Moreover, it has been reported that the tight binding of CaM to MLCK in the tissue does not require any Ca^{2+} bound to CaM [10]. At low $[\text{Ca}^{2+}]$, MLCK is present in complexes with Ca^{2+} -free CaM and Ca_2CaM . In the latter complex, Ca^{2+} is bound to the C-terminal of CaM since the affinity of these binding sites is increased by the presence of MLCK in the complex [10]. Neither of those two complexes is capable of activation of the MLCK [10,11]. In accordance with these findings, the Ca^{2+} /CaM activation of MLCK appears at sufficiently high Ca^{2+} levels, when in addition to the C-terminal binding sites, the N-terminal binding sites for Ca^{2+} on CaM are saturated as well. This induces an additional conformational change transmitted to activation of MLCK [4,10,11].

Here, we propose a model of a detailed kinetic scheme of interactions among Ca^{2+} , CaM and MLCK that takes into account different binding states of CaM with respect to the N- and C-terminal binding sites for Ca^{2+} and the binding site for MLCK. The mathematical model for the proposed kinetic scheme includes 24 kinetic constants in which the most recent and novel characteristics of binding properties between those species are reflected. Most of the parameter values are directly or indirectly based on experimental results, and some of them are predicted using the model constraints. The main purpose of constructing such a detailed model is to theoretically predict the concentration of active form of MLCK in dependence on $[\text{Ca}^{2+}]$. The model results are compared with the recently published quantitative measurement of Ca^{2+} /CaM binding and activation of MLCK [12]. Moreover, a detailed kinetic scheme enables an insight into how the various parameters governing individual reaction steps can affect the active form of MLCK. So, the robustness of the model is examined by applying an order of magnitude differences in the model parameter K_2 which represents the dissociation constant of MLCK for Ca_4CaM . In this way, the effect of phosphorylated MLCK on the model predictions is simulated as well.

2. Materials and methods

A theoretical approach is used for analyzing the interactions among Ca^{2+} , CaM and MLCK. The study is based on the mathematical model derived from the kinetic scheme of interactions presented in Fig. 1. In that figure and throughout the paper CaM represents

*Corresponding author. Fax: +386 2 251 81 80.

E-mail addresses: ales.fajmut@uni-mb.si (A. Fajmut), milan.brumen@uni-mb.si (M. Brumen), schuster@minet.uni-jena.de (S. Schuster).

Abbreviations: CaM, calmodulin; MLCK, myosin light chain kinase; MLC, myosin light chain; CaMKII, calmodulin kinase II

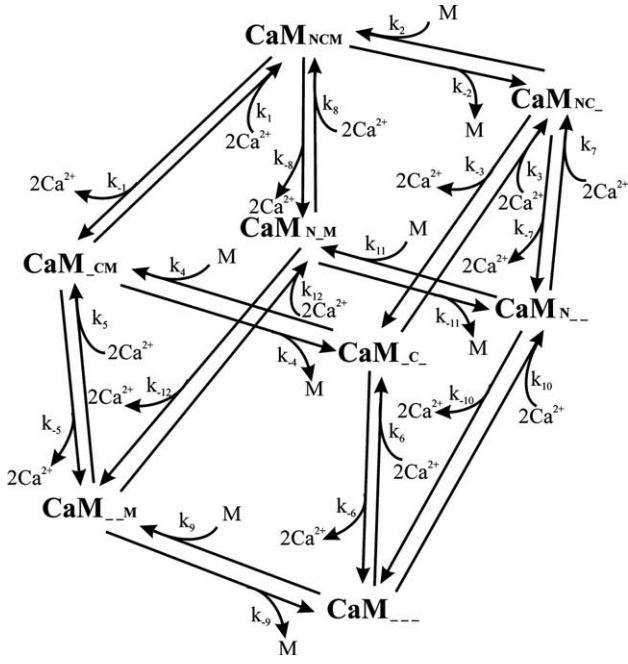


Fig. 1. Kinetic scheme of interactions between Ca^{2+} , CaM and MLCK. For symbols, see text.

calmodulin, the subscripts N and C represent the two binding sites at the N- and C-terminal of CaM, respectively, each occupied with a pair of Ca^{2+} ions, the subscript M represents the binding site on CaM occupied by MLCK, whereas an underscore (_) represents an unoccupied state at CaM for each of the above-mentioned binding sites. k_i and k_{-i} are the on and off rate constants, respectively. For example, the symbol $\text{CaM}_{N,M}$ represents the $\text{Ca}_2\text{CaM} \cdot \text{MLCK}$ complex with two Ca^{2+} ions bound to the N terminal of CaM.

Taking into account that there exist three independent binding sites on CaM, each of which may be empty or occupied, there exist 2^3 different species. In the scheme each of them is placed in a corner of the cube and connected with its three neighbors by the three two-way reactions along the edges of the cube. Thus, there are 12 different reactions with 24 rate constants in total.

There are nine variables in the mathematical model: All different states of the CaM molecule are represented by eight variables and the free MLCK concentration is another one, whereas $[\text{Ca}^{2+}]$ is considered as a parameter. We take into account the conservation relations (1) and (2) for CaM and MLCK concentrations, respectively, by which the number of the first-order ordinary differential equations describing the time evolution of the system reduces to seven equations, numbered (3)–(9):

$$[\text{CaM}_{_}] = [\text{CaM}_{\text{tot}}] - ([\text{CaM}_{N,C_}] + [\text{CaM}_{C,M}] + [\text{CaM}_{C_}] + [\text{CaM}_{_M}] + [\text{CaM}_{N_}] + [\text{CaM}_{N,M}] + [\text{CaM}_{NCM}]) \quad (1)$$

$$[M] = [M_{\text{tot}}] - ([\text{CaM}_{C,M}] + [\text{CaM}_{_M}] + [\text{CaM}_{N,M}] + [\text{CaM}_{NCM}]) \quad (2)$$

$$\frac{d[\text{Ca}_{CM}]}{dt} = -k_1[\text{Ca}^{2+}]^2[\text{Ca}_{CM}] + k_{-1}[\text{CaM}_{NCM}] + k_4[M][\text{CaM}_{C_}] - k_{-4}[\text{CaM}_{CM}] + k_5[\text{Ca}^{2+}]^2[\text{CaM}_{_M}] - k_{-5}[\text{CaM}_{CM}] \quad (3)$$

$$\frac{d[\text{CaM}_{NC_}]}{dt} = -k_2[M][\text{CaM}_{NC_}] + k_{-2}[\text{CaM}_{NCM}] + k_3[\text{Ca}^{2+}]^2[\text{CaM}_{C_}] - k_{-3}[\text{CaM}_{NC_}] + k_7[\text{Ca}^{2+}]^2[\text{CaM}_{n_}] - k_{-7}[\text{CaM}_{NC_}] \quad (4)$$

$$\frac{d[\text{CaM}_{C_}]}{dt} = -k_3[\text{Ca}^{2+}]^2[\text{CaM}_{C_}] + k_{-3}[\text{CaM}_{NC_}] - k_4[M] \times [\text{CaM}_{C_}] + k_{-4}[\text{CaM}_{CM}] + k_6[\text{Ca}^{2+}]^2[\text{CaM}_{_}] - k_{-6}[\text{CaM}_{C_}] \quad (5)$$

$$\frac{d[\text{CaM}_{_M}]}{dt} = -k_5[\text{Ca}^{2+}]^2[\text{CaM}_{_M}] + k_{-5}[\text{CaM}_{CM}] + k_9[M] \times [\text{CaM}_{_}] - k_{-9}[\text{CaM}_{_M}] - k_{12}[\text{Ca}^{2+}]^2[\text{CaM}_{_M}] + k_{-12}[\text{CaM}_{N,M}] \quad (6)$$

$$\frac{d[\text{CaM}_{N_}]}{dt} = -k_7[\text{Ca}^{2+}]^2[\text{CaM}_{N_}] + k_{-7}[\text{CaM}_{NC_}] + k_{10}[\text{Ca}^{2+}]^2 \times [\text{CaM}_{_}] - k_{-10}[\text{CaM}_{N_}] - k_{11}[M][\text{CaM}_{N_}] + k_{-11}[\text{CaM}_{N,M}] \quad (7)$$

$$\frac{d[\text{CaM}_{N,M}]}{dt} = -k_8[\text{Ca}^{2+}]^2[\text{CaM}_{N,M}] + k_{-8}[\text{CaM}_{NCM}] + k_{11}[M] \times [\text{CaM}_{N_}] - k_{-11}[\text{CaM}_{N,M}] + k_{12}[\text{Ca}^{2+}]^2[\text{CaM}_{_M}] - k_{-12}[\text{CaM}_{N,M}] \quad (8)$$

$$\frac{d[\text{CaM}_{NCM}]}{dt} = +k_1[\text{Ca}^{2+}]^2[\text{CaM}_{CM}] - k_{-1}[\text{CaM}_{NCM}] + k_2[M][\text{CaM}_{NC_}] - k_{-2}[\text{CaM}_{NCM}] + k_8[\text{Ca}^{2+}]^2[\text{CaM}_{N,M}] + k_{-8}[\text{CaM}_{NCM}] \quad (9)$$

The steady states of the system variables with respect to different $[\text{Ca}^{2+}]$ are found by integration of the dynamical system at the initial condition $[\text{CaM}_{_}] = [\text{CaM}_{\text{tot}}]$ until the relative changes in all variables over 10^3 time steps are smaller than 10^{-6} . Integration is carried out in Berkeley Madonna 8.0 with the Runge–Kutta 4 integration method. The numerical simulations show that the steady-state values are attained in a monotonic or biphasic way. This is understandable because the steady state is here a thermodynamic equilibrium state.

In our model, we take into account binding of two Ca^{2+} ions to CaM, hence, the on-rate constant is defined as $k_i = k_{-i}/K_i^2$, where k_{-i} is the off-rate constant and K_i is the dissociation constant. Therefore, the relation between the model parameter k_i and experimental values of the apparent on-rate constant k_i^{app} , defined in [8,13,14] as $k_i^{\text{app}} = k_{-i}/K_i$, is $k_i = k_i^{\text{app}}/K_i$.

The values for the dissociation and off-rate constants can be found in the literature, although for some reaction steps the data were limited. The unknown values were predicted by applying the so-called detailed balance or Wegscheider's condition valid in closed reaction systems [15,16]:

$$\prod_j K_j = 1, \quad (10)$$

where K_j denotes either K_i or K_i^2 , depending on the reaction considered. The first one corresponds to the binding of MLCK to CaM and the second one to the binding of two Ca^{2+} ions to CaM, respectively. For the subsequent analysis, we introduce the notation $K_i^2 = K_i^*$.

The kinetic scheme (Fig. 1) involves six basic closed cycles around each of the cube's planes. To all of these, Wegscheider's condition can be applied. All other more complex cycles are only a superposition of the former ones. The equations describing all six closed cycles are: $K_1^{-1}K_2K_3K_4^{-1} = 1$, $K_1^{-1}K_8^*K_9^*K_5^{-1} = 1$, $K_2^{-1}K_8^*K_{11}K_7^{-1} = 1$, $K_3^{-1}K_7^*K_{10}K_6^{-1} = 1$, $K_4^{-1}K_5^*K_9K_6^{-1} = 1$, $K_9^{-1}K_{10}^*K_{11}K_{12}^{-1} = 1$. Importantly, they can be reduced to five equations due to the conservation of total $[\text{CaM}]$. This follows from the reasoning that there are 12 reactions and seven independent concentration variables in the cube and the number of degrees of freedom in fluxes equals the difference between these two values [15]. Using Wegscheider's condition we express the parameters K_4 , K_5^* , K_9 , K_{10}^* and K_{11} as the unknown quantities. Concomitantly, by taking into account the known values of the corresponding off-rate constants and the on-rate constants were calculated. Due to lack of information, for the value k_{11} (see Table 2) a similar value was taken as in all reactions considering the binding of MLCK to CaM.

The experimental results for the dissociation and off-rate constants are, in many cases, very diverse, as the experiments are often performed on peptides containing a core CaM binding sequences of the smooth- or skeletal-muscle MLCK and sometimes even on a genetically engineered CaM with binding properties much different from native CaM [8,9,14,17–21]. Generally, Ca^{2+} binding to CaM that is complexed with MLCK is studied in much more detail in the cases when the full-length protein is replaced by the CaM target peptide of that specific protein; nevertheless our model parameters resemble the properties of intact MLCK. Furthermore, parameter values emerge from different experiments, and, in the model, the equilibrium constants are subject to the Wegscheider's condition (note that a change in one parameter affects at least one other parameter due to this constraint). Therefore, a direct transfer of the parameter values from the references into our model has to undergo an additional tuning of the values. A complete and coherent set of the model parameters and their values is presented in Tables 1 and 2. It is based on the study of kinetic properties of interactions among Ca^{2+} , CaM and MLCK, experimental observations of which are given in the references listed also in Tables 1 and 2. These kinetic properties are summarized in the following:

- The MLCK affinity for Ca_4CaM is in the nM range, whereas the affinity for Ca_2CaM is lower. A typical K_d value of unphosphorylated MLCK for Ca_4CaM is around 1 nM [9,17,19,22,23]. Refs. [24,25] reported a 10-fold smaller K_d . In the reference state of our model $K_2 = 1$ nM; K_4 and K_{11} are approximately 5-fold larger.
- The intact full-length MLCK increases an apparent affinity of CaM for Ca^{2+} to a significantly smaller extent than does isolated target peptide [14]. In our model, the apparent affinities were calculated for the reaction schemes presented on the corresponding right and left vertical planes in the kinetic scheme in Fig. 1 and they differ 8-fold (calculation not shown). This is significantly smaller than the 44-fold difference reported for smooth-muscle MLCK-peptide [14].
- The C-terminal affinity for Ca^{2+} in the absence of MLCK is approximately 1.5 μM and is approximately 2–4 times higher than for the N-terminal [8,26]. Note that $K_6 = K_7 = 1.46$ μM and $K_{10}/K_6 \approx 1.9$. In the presence of MLCK, the C-terminal affinity for Ca^{2+} is approximately 10-fold lower [8]. Note that $K_6/K_5 = K_7/K_8 \approx 14.6$.
- Ca^{2+} apparently binds approximately 70-fold faster to the N-terminal than to the C-terminal [8,27]. Note that $k_6^{\text{app}}/k_{10}^{\text{app}} = k_7^{\text{app}}/k_3^{\text{app}} \approx 69$.
- The presence of MLCK slows down the Ca^{2+} dissociation from the C-terminal by approximately 30–50 times [8,9] ($k_{-7}/k_{-8} = k_{-6}/k_{-5} = 30$) and from the N-terminal by 140–225 times [8,14] ($k_{-3}/k_{-1} = k_{-10}/k_{-12} = 200$).

Table 1
Model parameters concerning Ca^{2+} binding to CaM

i	K_i (μM)	K_i^* (μM^2)	k_i ($\mu\text{M}^{-2} \text{s}^{-1}$)	k_{-i} [s^{-1}]	References
1	0.365	0.133	30.0	4.00	[9,17,19]
3	2.83	8.00	100	800	[8,9,13,18,20,26,27,32]
5	0.10	0.010	20	0.20	[8,9]
6	1.46	2.14	2.80	6.00	[8,9,13,18,20,27,32]
7	1.46	2.14	2.80	6.00	[8,9,13,18,20,27,32]
8	0.20	0.040	5.0	0.20	[8]
10	2.83	8.00	100	800	[8,9,13,18,20,27,32]
12	0.182	0.0333	120	4.00	[27]

Table 2
Model parameters concerning MLCK binding to CaM

i	K_i (μM)	k_i ($\mu\text{M}^{-1} \text{s}^{-1}$)	k_{-i} (s^{-1})	References
2	0.001	1000	1	[9,17,19,22–25]
4	0.060	1000	60	[9]
9	12.8	910	11700	[9,21,28]
11	0.054	840	45	(see text)

- In the presence of MLCK, Ca^{2+} dissociates 15–30 times faster from the N-terminal than from the C-terminal [8,14]. Note that $k_{-1}/k_{-8} = k_{-12}/k_{-5} = 20$.
- The half-saturation constant of Ca^{2+} binding to the C-terminal is approximately 1.5 μM in the absence of MLCK, whereas in the presence of MLCK this parameter is approximately 10-fold lower [8]. Note that $K_6/K_5 = K_7/K_8 \approx 14.6$.
- The effect of the MLCK on the N- and C-terminal Ca^{2+} affinities is approximately equal [9]. Note that $K_6/K_5 \approx K_{10}/K_{12}$ and $K_7/K_8 \approx K_3/K_1$.
- The MLCK affinity for Ca^{2+} -free CaM is very low compared to the affinity for Ca_2CaM and Ca_4CaM and is in the range $K_d = 1$ $\mu\text{M} \dots 270$ μM [9,21,28]. $K_9 = 12.8$ μM in our model.

Following the experimental conditions in Ref. [12], we first used 10 and 2 μM for the total [CaM] and total [MLCK] values, respectively. This is in accordance with the concentrations measured in smooth muscles [29–31]. It is an open question how much of the total [CaM] is bound to proteins other than MLCK in the cell. A rough estimate can be, that as much would remain for binding to MLCK, as there is total [MLCK]. Therefore, we repeated the simulations with a total [CaM] of 2 μM and compared the results.

3. Results and discussion

Ca^{2+} /CaM-dependent activation of MLCK has been studied in terms of mathematical modeling only in few cases. In 1984 Kato et al. [33] proposed a two-step kinetic model among Ca^{2+} , CaM and MLCK. The approach in which the authors considered that only the Ca_4CaM complex could bind to and activate MLCK was based on the rapid equilibrium approximation. The interaction between the Ca^{2+} /CaM complex and MLCK at high saturating [Ca^{2+}] was studied theoretically and experimentally by Török and coworkers [24,25] under conditions when MLCK was either free or in a steady-state complex with the substrate MLC. Very recently Lukas [28] proposed a more detailed, four-step kinetic model of interactions between Ca^{2+} , CaM and MLCK. However, details such as different binding properties of the N- and C-terminals of CaM were not taken into consideration. A cube-like reaction scheme similar to ours was already proposed by Brown et al. [9]. Their analysis was aimed at studying the various dissociation pathways of the CaM/MLCK-peptide complex, and only five dissociation reactions were considered in their model.

Recently, MLCK activation was quantitatively examined in vitro by a fluorescent biosensor of MLCK, where a Ca^{2+} dependent increase in kinase activity was coincidental with a decrease in fluorescence resonance energy transfer (FRET) [12]. A FRET signal is a measure of Ca^{2+} /CaM binding to MLCK, in particular of $\text{Ca}_4\text{CaM} \cdot \text{MLCK}$ and probably also of $\text{Ca}_2\text{CaM} \cdot \text{MLCK}$ complexes [12]. Due to a similar dependence of myosin light chain phosphorylation it was proposed that it could be a measure of MLCK activity [12]. Additionally, these data are in agreement with experimental data on Ca^{2+} -dependent MLCK activity [34]. In order to compare the experimental findings with our model predictions we define two variables, A and F , to quantify the active form of MLCK and FRET dependence on [Ca^{2+}], respectively. They are defined as:

$$A = \frac{[\text{CaM}_{\text{NCM}}]}{[\text{M}_{\text{tot}}]} \quad (11)$$

$$F = \frac{[\text{CaM}_{\text{NCM}}] + [\text{CaM}_{\text{CM}}] + [\text{CaM}_{\text{NCM}}]}{[\text{M}_{\text{tot}}]} \quad (12)$$

and have values between 0 and 1.

In Fig. 2(A) and (B), we compare the model predictions (curves) for variables A and F versus $[Ca^{2+}]$ with the Ca^{2+} -dependent FRET signal acquired from Fig. 3A (open circles) in [12]. The experimental data were transferred by using the Digitizer tool in Origin 6.1. Note that the curves for F always lie above the graph for A , as it should be because Eqs. (11) and (12) imply $F > A$.

Fig. 2A shows the model predictions at two different total $[CaM]$ values, 2 and 10 μM . The difference between F and A at the same total $[CaM]$ is remarkable, indicating that the concentrations of both $[CaM_{CM}]$ and $[CaM_{NM}]$ species is non-negligible. This is in favor of the presence of $Ca_2CaM \cdot MLCK$ complexes already at low $[Ca^{2+}]$ [8,10]. Fig. 2A also indicates that the best match to the experimental data based upon in vitro FRET experiments [12] is that one with $[CaM_{tot}] = 2 \mu M$. The parameter values presented in Tables 1 and 2 and the total concentrations of $[CaM]$ and $[MLCK]$ equal to 2 μM thus represent the reference state of the model.

It is worthwhile emphasizing that the curves were not fitted to the experimental data. They are predictions of the model that emerge from adjustment of the parameter values and their ratios within the reasonable range of known experimental data. The parameter values reflect the properties of smooth-

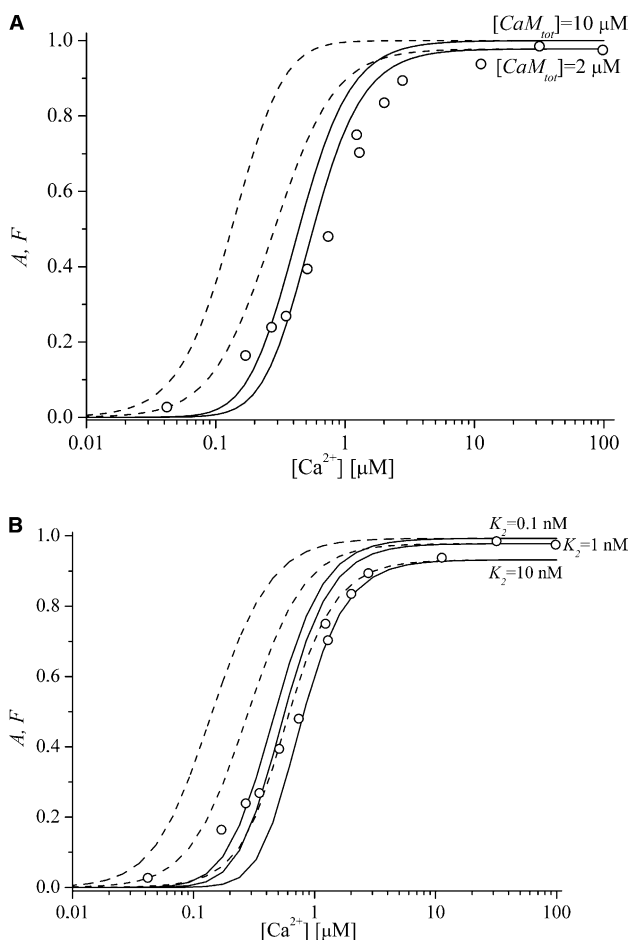


Fig. 2. Predictions of the model variables A (solid line) and F (dashed line) versus $[Ca^{2+}]$. (A) At the total $[CaM]$ of 2 and 10 μM , $K_2 = 1$ nM. (B) At $K_2 = 0.1, 1, 10$ nM, $K_4 = 6, 60, 600$ nM, $K_9 = 1.28, 12.8, 128 \mu M$, $K_{11} = 5.4, 54, 540$ nM, respectively, $[CaM_{tot}] = [MLCK_{tot}] = 2 \mu M$. Experimental data (open circles) from Fig. 3A in [12].

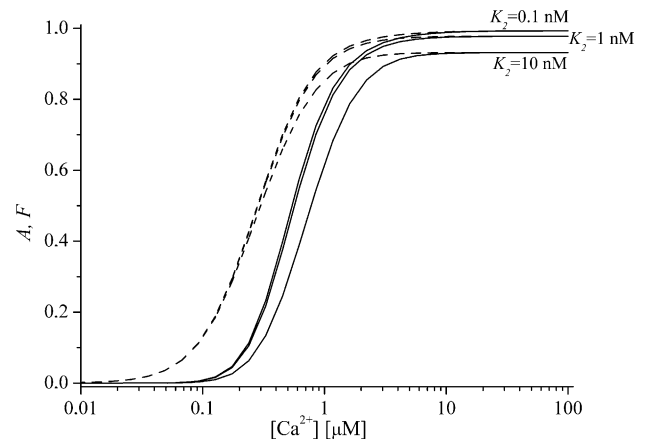


Fig. 3. Predictions of the model variables A (solid line) and F (dashed line) versus $[Ca^{2+}]$ at $K_2 = 0.1, 1, 10$ nM, $[CaM_{tot}] = [MLCK_{tot}] = 2 \mu M$. All other parameter values are the same as in Tables 1 and 2. The system reference state is represented by curves with $K_2 = 1$ nM.

muscle MLCK rather than of MLCK-peptide analogues or other MLCK isoforms although some of them were consulted in adjusting the parameter values. Constraints like the Wegscheider's condition and some ratios between certain parameter values were applied to preserve the relations between the values, and some unknown parameter values were also predicted (Tables 1 and 2).

The present mathematical model of interactions between Ca^{2+} , CaM and MLCK explicitly ignores the presence of the substrate MLC, its phosphorylation and the phosphorylation of CaM and MLCK. These simplifications restrict the applicability of the model predictions in discussing experimental observations in vivo as well as in vitro. In the following, the effect the model parameter K_2 has on the model predictions will be discussed. In our model scheme, the parameter K_2 represents the dissociation constant of MLCK for Ca_4CaM . There is a diversity of values of this dissociation constant reported in the literature; values around 0.1 nM [24,25] and in the range between 0.5 and 1 nM [9,17,19,22,23] are given for full-length MLCK, values ranging from 0.1 to 20 nM were observed for interactions between Ca_4CaM and MLCK-peptides [9,24], and the values 6 and 20 nM were reported for Ca_4CaM binding to phosphorylated MLCK [19,35].

Since the equilibrium constants are subject to the Wegscheider's condition, a change in one-parameter value affects at least one other parameter. The selection of parameters that are affected by a change in K_2 is not unique; we apply the Wegscheider's condition in such a way that it does not affect the ratios among the parameter values described in Section 2. Note that it would not be sufficient to change one parameter in addition to K_2 because K_2 enters two cycles and because the change in another dissociation constant affects further cycles. A change of a minimum number of constants is achieved by expressing the parameters K_4, K_9, K_{11}, K_5^* and K_{10}^* explicitly by others, whereby only the parameters related to CaM binding to MLCK (K_4, K_9, K_{11}) are affected after a change in K_2 . Thus, a 10-fold increase (or decrease) in K_2 induces a 10-fold increase (or decrease) in these parameter values. Fig. 2B shows the model predictions obtained by changing the parameter values as described. The total $[CaM]$ and $[MLCK]$ are taken to be

equal to 2 μM . Significant (2-fold) shifts in the half-saturation values of the variable F with respect to the reference state ($K_2 = 1 \text{ nM}$) can be observed. However, the half-saturation values for the variable A and the maximal values for A as well as for F are not affected that much. A 10-fold increase in the selected parameter values results in a 40% increase of the apparent half-saturation value for variable A with respect to the reference state, and in a decrease of maximal value of both variables for about 5%.

The comparison of different saturation levels of the active form of MLCK in Fig. 2A at two different total $[\text{CaM}]$ of 2 and 10 μM shows that at the lower total $[\text{CaM}]$ which equals the total $[\text{MLCK}]$, not all of the MLCK is activated. Similar feature was observed in recent studies on MLCK sensor proteins [12]. This system property is in our model even more pronounced when the total $[\text{CaM}]$ is lower than the total $[\text{MLCK}]$ (data not shown). These findings are more visible under conditions of 10-fold increased K_2 values (see Fig. 2B). Such a high value (10 nM) roughly corresponds to the K_d of phosphorylated MLCK for Ca_4CaM [19].

It is well established that protein kinase A (PKA), protein kinase G and calmodulin kinase II (CaMKII) phosphorylate MLCK (reviewed in [36]). In our model, however, phosphorylation of MLCK is not explicitly taken into consideration but it can be discussed along with an order of magnitude changes in parameter values concerning the $\text{Ca}^{2+}/\text{CaM}$ binding to MLCK. This approach is oversimplified as it is known that MLCK phosphorylation and thus K_d could be Ca^{2+} dependent as well [37]. The values for K_d reported in vivo range between 1 and 7 nM under physiological $[\text{Ca}^{2+}]$ [37], whereas in vitro data reported in [35] and [19] are 6.4 and 20 nM, respectively, under conditions of high saturating $[\text{Ca}^{2+}]$. Thus, in our model, the latter values correspond to binding of the Ca_4CaM complex to MLCK. As MLCK can be phosphorylated only if it does not contain bound CaM [35,37] it is possible that the affinities of MLCK for Ca_2CaM and Ca^{2+} -free CaM species and thus parameters K_4 , K_{11} and K_9 are affected as well. It seems therefore reasonable to raise the question how the binding of Ca_2CaM species and Ca^{2+} -free CaM to MLCK is affected by MLCK phosphorylation. Fig. 2B shows the effects of an order of magnitude changes in all these parameter values on the active form of MLCK. However, any final answer will be doubtful as the influence of phosphorylated MLCK on the parameter values K_4 , K_9 and K_{11} should be clarified first.

Additionally, we present the effect of changing solely K_2 on the model predictions. In principle, this procedure violates the equilibrium Wegscheider's condition, but non-equilibrium conditions in vivo could argue for presenting the response of the model upon such a perturbation. In Fig. 3, we present predictions for model variables A and F by modifying the parameter value K_2 10-fold higher and lower with respect to the reference value of 1 nM whereby all other parameter values are the same as in the reference state. Total $[\text{CaM}]$ is taken to be equal to 2 μM . The results clearly indicate that the influence of K_2 increases with its absolute value.

Ikebe and Reardon [35] studied MLCK phosphorylation by CaMKII in vitro under conditions $[\text{CaM}] = 20 \mu\text{M}$, $[\text{MLCK}] = 10 \mu\text{M}$ and $[\text{Ca}^{2+}] = 100 \mu\text{M}$, and showed that the maximum rate of kinase activity (V_{max}) was not affected by MLCK phosphorylation. The K_d of phosphorylated MLCK for $\text{Ca}^{2+}/\text{CaM}$ predicted under these experimental conditions was 6.4 nM in the absence of bound CaM to MLCK. Our

model simulation under conditions $[\text{CaM}_{\text{tot}}] = 20 \mu\text{M}$, $[\text{MLCK}_{\text{tot}}] = 10 \mu\text{M}$ and $K_2 = 6.4 \text{ nM}$ indicates that all MLCK is in its active form at high saturating $[\text{Ca}^{2+}] = 100 \mu\text{M}$ (data not explicitly shown).

In summary, a simple view that after an increase in $[\text{Ca}^{2+}]$, Ca^{2+} ions bind to four-binding sites of Ca^{2+} -free CaM, and that only the Ca_4CaM complex interacts with and activates MLCK, was recently improved and broadened by the fact that also Ca^{2+} -free CaM as well as all various Ca^{2+} -bound CaM species can interact with MLCK. Recent experiments also show much different rates and affinities for Ca^{2+} binding to CaM when CaM is associated with MLCK. In this case, the Ca^{2+} binding affinity to the C-terminal binding sites of CaM is enhanced approximately 10-fold [8] and both C- and N-terminal dissociation rates for Ca^{2+} are decreased approximately by a factor of 30 and 150, respectively [8,9]. Following these new findings, we here presented a novel complex kinetic scheme of interactions among Ca^{2+} , CaM and MLCK and modeled it by a dynamical system. A dynamic approach is particularly important in the case when the Ca^{2+} input signal would be considered as a variable. Such an approach will be necessary as the time scale of particular reactions in the proposed model is similar to the characteristic time of Ca^{2+} transients in cytosolic Ca^{2+} oscillations observed in smooth muscle cells [38].

Acknowledgments: The authors gratefully acknowledge a travel grant from the Slovenian and German Ministries of Research and Education (Grant Nos. BI-DE/03-04-003 and SVN 02/013, respectively) for mutual working visits.

References

- [1] Kamm, K.E. and Stull, J.T. (2001) Dedicated myosin light chain kinases with diverse cellular functions. *J. Biol. Chem.* 276, 4527–4530.
- [2] Dabrowska, R., Hinkins, S., Walsh, M.P. and Hartshorne, D.J. (1982) The binding of smooth-muscle myosin light chain kinase to actin. *Biochem. Biophys. Res. Commun.* 107, 1524–1531.
- [3] Smith, L. and Stull, J.T. (2000) Myosin light chain kinase binding to actin filaments. *FEBS Lett.* 480, 298–300.
- [4] Allen, B.G. and Walsh, M.P. (1994) The biochemical basis of the regulation of smooth-muscle contraction. *Trends Biochem. Sci.* 19, 362–368.
- [5] Somlyo, A.P. and Somlyo, A.V. (1994) Signal transduction and regulation in smooth muscle. *Nature* 372, 231–236.
- [6] Smith, P.G., Roy, C., Dreger, J. and Brozovich, F. (1999) Mechanical strain increases velocity and extent of shortening in cultured airway smooth muscle cells. *Am. J. Physiol. Lung Cell Mol. Physiol.* 277, L343–L348.
- [7] Skloot, G., Permutt, S. and Togias, A. (1995) Airway hyperresponsiveness in asthma: a problem of limited smooth muscle relaxation with inspiration. *J. Clin. Invest.* 96, 2393–2403.
- [8] Johnson, J.D., Snyder, C., Walsh, M. and Flynn, M. (1996) Effects of myosin light chain kinase and peptides on Ca^{2+} exchange with the N- and C-terminal Ca^{2+} binding sites of calmodulin. *J. Biol. Chem.* 271, 761–767.
- [9] Brown, S.E., Martin, S.R. and Bayley, P.M. (1997) Kinetic control of the dissociation pathway of calmodulin-peptide complexes. *J. Biol. Chem.* 272, 3389–3397.
- [10] Wilson, D.P., Sutherland, C. and Walsh, M.P. (2002) Ca^{2+} activation of smooth muscle contraction. Evidence for the involvement of calmodulin that is bound to the triton-insoluble fraction even in the absence of Ca^{2+} . *J. Biol. Chem.* 277, 2186–2192.
- [11] Krueger, J.K., Gallagher, S.C., Zhi, G., Geguchadze, R., Persechini, A., Stull, J.T. and Trewella, J. (2001) Activation of

- Myosin Light Chain Kinase Requires Translocation of Bound Calmodulin. *J. Biol. Chem.* 276, 4535–4538.
- [12] Geguchadze, R., Zhi, G., Lau, K.S., Isotani, E., Persechini, A., Kamm, K.E. and Stull, J.T. (2004) Quantitative measurements of Ca^{2+} /calmodulin binding and activation of myosin light chain kinase in cells. *FEBS Lett.* 557, 121–124.
- [13] Falke, J.J., Drake, S.K., Hazard, A.L. and Peersen, O.B. (1994) Molecular tuning of ion-binding to calcium signaling proteins. *Q. Rev. Biophys.* 27, 219–290.
- [14] Peersen, O.B., Madsen, T.S. and Falke, J.J. (1997) Intermolecular tuning of calmodulin by target peptides and proteins: Differential effects on Ca^{2+} binding and implications for kinase activation. *Protein Sci.* 6, 794–807.
- [15] Heinrich, R. and Schuster, S. (1996) The regulation of cellular systems, Chapman & Hall, New York.
- [16] Hearon, J.Z. (1953) The kinetics of linear systems with special reference to periodic reactions. *Bull. Math. Biophys.* 15, 121–141.
- [17] Johnson, J., Holroyde, M., Crouch, T., Solaro, R. and Potter, J. (1981) Fluorescence studies of the interaction of calmodulin with myosin light chain kinase. *J. Biol. Chem.* 256, 12194–12198.
- [18] Bayley, P.M., Ahlström, P., Martin, S.R. and Forsén, S. (1984) The kinetics of calcium binding to calmodulin: Quin 2 and ANS stopped-flow fluorescence studies. *Biochem. Biophys. Res. Commun.* 120, 185–191.
- [19] Kasturi, R., Vasulka, C. and Johnson, J. (1993) Ca^{2+} , caldesmon, and myosin light chain kinase exchange with calmodulin. *J. Biol. Chem.* 268, 7958–7964.
- [20] Yang, J.J., Gawthrop, A. and Ye, Y. (2003) Obtaining site-specific calcium-binding affinity of calmodulin. *Protein Pept. Lett.* 10, 331–345.
- [21] Tsvetkov, P.O., Protasevich, I.I., Gilli, R., Lafitte, D., Lobachov, V.M., Haiech, J., Briand, C. and Makarov, A.A. (1999) Apocalmodulin binds to the myosin light chain kinase calmodulin target site. *J. Biol. Chem.* 274, 18161–18164.
- [22] Blumenthal, D. and Stull, J. (1980) Activation of skeletal muscle myosin light chain kinase by calcium(2+) and calmodulin. *Biochemistry* 19, 5608–5614.
- [23] Gallagher, P., Herring, B., Trafny, A., Sowadski, J. and Stull, J. (1993) A molecular mechanism for autoinhibition of myosin light chain kinases. *J. Biol. Chem.* 268, 26578–26582.
- [24] Török, K., Cowley, D., Brandmeier, B., Howell, S., Aitken, A. and Trentham, D. (1998) Inhibition of calmodulin-activated smooth-muscle myosin light-chain kinase by calmodulin-binding peptides and fluorescent (phosphodiesterase-activating) calmodulin derivatives. *Biochemistry* 37, 6188–6198.
- [25] Török, K. and Trentham, D.R. (1994) Mechanism of 2-chloro-(epsilon-amino-Lys75)-[6-[4-(N,N-diethylamino)phenyl]-1,3,5-triazin-4-yl]calmodulin interactions with smooth muscle myosin light chain kinase and derived peptides. *Biochemistry* 33, 12807–12820.
- [26] Minowa, O. and Yagi, K. (1984) Calcium binding to tryptic fragments of calmodulin. *J. Biochem. (Tokyo)* 56, 1175–1182.
- [27] Persechini, A., Yano, K. and Stemmer, P.M. (2000) Ca^{2+} binding and energy coupling in the calmodulin-myosin light chain kinase complex. *J. Biol. Chem.* 275, 4199–4204.
- [28] Lukas, T.J. (2004) A signal transduction pathway model prototype I: from agonist to cellular endpoint. *Biophys. J.* 87, 1406–1416.
- [29] Tansey, M., Luby-Phelps, K., Kamm, K. and Stull, J. (1994) Ca^{2+} -dependent phosphorylation of myosin light chain kinase decreases the Ca^{2+} sensitivity of light chain phosphorylation within smooth muscle cells. *J. Biol. Chem.* 269, 9912–9920.
- [30] Zimmermann, B., Somlyo, A.V., Ellis-Davies, G.C.R., Kaplan, J.H. and Somlyo, A.P. (1995) Kinetics of prephosphorylation reactions and myosin light chain phosphorylation in smooth muscle. Flash photolysis studies with caged calcium and caged ATP. *J. Biol. Chem.* 270, 23966–23974.
- [31] Szymanski, P.T., Szymanska, G. and Goyal, R.K. (2002) Differences in calmodulin and calmodulin-binding proteins in phasic and tonic smooth muscles. *Am. J. Physiol. Cell Physiol.* 282, C94–C104.
- [32] Martin, S.R., Maune, J.F., Beckingham, K. and Bayley, P.M. (1992) Stopped-flow studies of calcium dissociation from calcium-binding-site mutants of *Drosophila melanogaster* calmodulin. *Eur. J. Biochem.* 205, 1107–1114.
- [33] Kato, S., Osa, T. and Ogasawara, T. (1984) Kinetic model for isometric contraction in smooth muscle on the basis of myosin phosphorylation hypothesis. *Biophys. J.* 46, 35–44.
- [34] Van Lierop, J.E., Wilson, D.P., Davis, J.P., Tikunova, S., Sutherland, C., Walsh, M.P. and Johnson, J.D. (2002) Activation of smooth muscle myosin light chain kinase by calmodulin. Role of LYS30 and GLY40. *J. Biol. Chem.* 277, 6550–6558.
- [35] Ikebe, M. and Reardon, S. (1990) Phosphorylation of smooth muscle myosin light chain kinase by smooth muscle Ca^{2+} /calmodulin-dependent multifunctional protein kinase. *J. Biol. Chem.* 265, 8975–8978.
- [36] Pfitzer, G. (2001) Signal transduction in smooth muscle: invited review: Regulation of myosin phosphorylation in smooth muscle. *J. Appl. Physiol.* 91, 497–503.
- [37] Tang, D., Stull, J., Kubota, Y. and Kamm, K. (1992) Regulation of the Ca^{2+} dependence of smooth muscle contraction. *J. Biol. Chem.* 267, 11839–11845.
- [38] Hyvelin, J.M., Roux, E., Prevost, M.C., Savineau, J.P. and Marthan, R. (2000) Cellular mechanisms of acrolein-induced alteration in calcium signaling in airway smooth muscle. *Toxicol. Appl. Pharmacol.* 164, 176–183.